Production of neutron-rich Bi isotopes by transfer reactions

K. Eskola,* P. Eskola,† M. M. Fowler, H. Ohm, E. N. Treher,‡ and J. B. Wilhelmy
Los Alamos National Laboratory, Los Alamos, New Mexico 87545

D. Lee and G. T. Seaborg
Lawrence Berkeley Laboratory, Berkeley, California 94720
(Received 7 December 1983)

Production of neutron-rich Bi isotopes was investigated by irradiating Hg, Tl, and Pb targets with ^{18}O ions in the 5—10 MeV/nucleon range. Following irradiation, bismuth was chemically separated and the yields of $^{211-213}$Bi isotopes were determined via α-emitting Po daughters. Effective residual transfers of $^{3-5}$H to ^{208}Pb, ^{7,8}He to ^{205}Tl, and ^{8}Li to ^{204}Hg were observed. Cross sections generally peaked in the 7—8 MeV/nucleon region and ranged from a high of $\sim$2 mb for ^{3}He absorption to $\sim$0.6 nb for ^{8}He absorption. Total α- and β-decay branches of the $J^{\pi}=9^{-}$, 25 min isomer of ^{212}Bi were measured to be 67% and 33%, respectively, (3.2±0.2)% of the decays being associated with β-delayed α-particle emission. Production yields for the $J^{\pi}=1^{-}$ ground state and 9^{-} and 15^{-} isomeric levels for ^{212}Bi were extracted. The ratio of isomeric states to the ground state increased by more than two orders of magnitude over the energy range studied. However, the maximum value of the cross section ratio $\sigma(J^{\pi}=15^{-})/\sigma(J^{\pi}=9^{-})$ was only 0.04, implying a low angular momentum transfer. The reactions were analyzed using the Wilczyński "sum rule," which gave a rather poor fit to the results with respect to both the yield and the implied angular momentum transfer. The observed relatively high cross sections, modest angular momentum transfer, and broad excitation functions indicate that transfer processes provide a viable method for reaching neutron-rich nuclides in the heavy element region.

I. INTRODUCTION

The production of neutron excess isotopes is, in general, very difficult. Experimental results on the fission properties of the heavy isotopes in the Fm region[1-3] have shown very anomalous decay properties. Extended access into this interesting region will depend on developing techniques to produce these neutron-rich species. A possible method for reaching the desired products is through the use of transfer reactions in which more neutrons than protons are transferred to the heavy element target. Such transfers are not generally favored by the potential energy surface and therefore have small probability amplitudes. However, these reactions, when they do occur, have large negative Q values and can result in a relatively cold formation of the heavy element products which helps minimize the disastrous fission-neutron decay competition which occurs in most compound reaction processes in the region. On the other hand, a disadvantage for transfer reactions is that they are nonselective and result in a large variety of products which have to be disentangled with physical and/or chemical procedures.

The purpose of the current measurements is to study the production mechanism for these rather rare reaction processes. These reactions are not expected to be dominated by statistical effects, and therefore, we have attempted to study the excitations functions over a wide energy interval. To avoid the difficulties associated with the handling and analysis of the heavy actinide region we have chosen to produce isotopes of $^{211-213}$Bi formed in the bombardment of Hg, Tl, and Pb targets with ^{18}O beams. This is a convenient system for analysis since the produced neutron excess isotopes have half-lives in the minutes range and can be identified by characteristic α-particle emission in their decay sequence. High sensitivity can be obtained through chemical isolation of the desired products in rapid off-line analysis of reasonably thick irradiated targets. By studying the production properties in this more accessible region it is hoped that we can obtain systematic information on the mechanisms associated with the rare neutron excess production processes and thus gain a possible technique to enable future production of neutron-rich heavy actinides. In addition, these studies provide nuclear spectroscopic information regarding the region in the vicinity of the doubly magic ^{208}Pb.

II. EXPERIMENTAL PROCEDURE

A. Irradiations and targets

Irradiations of Hg, Tl, and Pb targets were performed at the Lawrence Berkeley Laboratory 88-inch cyclotron with 99—195 MeV ^{18}O ions. Irradiation times were typically 1—2 h, and the beam intensity ranged from 1.5 to 4 $e\mu$A but for each irradiation was kept approximately constant. The lead targets were enriched in ^{208}Pb (98.7%) with thicknesses ranging from 3.4 to 4.0 mg/cm^2, and the thallium targets were enriched in ^{205}Tl (99.4%) with thicknesses ranging from 4.3 to 4.8 mg/cm^2. In the case of mercury, targets of both natural isotopic composition and those enriched in ^{204}Hg (98.2%) were used. The thicknesses of the natural targets were 0.6—0.8 mg/cm^2

and those of enriched targets 0.2—0.8 mg/cm^2. In both cases the values refer to the chemical compound HgS, the form in which Hg was used. All the targets had thin Al coatings of 0.4—0.7 mg/cm^2 and thicker Al backings (2.17 mg/cm^2) to stop the recoiling reaction products.

B. Chemical procedures

The chemical procedure used to separate bismuth isotopes after irradiation was similar for all of the targets. The targets were dissolved in ~0.5 ml warm acid containing a known quantity of 38-yr ^{207}Bi for chemical yield determination. Concentrated HCl containing a few drops of 6M HNO_3 was used to dissolve the Pb and Tl targets, and aqua regia was used for the HgS targets.

Following target dissolution the samples were evaporated to dryness. The residues were taken up in ~$\frac{1}{2}$ ml 1M HCl. $PbCl_2$ formed from the lead targets and Hg_2Cl_2 precipitated from the mercury target solutions after addition of a couple of drops of $SnCl_2$ (2—5 mg) solution. A major At contamination, observed after processing of the Tl targets, was substantially reduced by coprecipitation with $PbCl_2$.

After centrifuging and removing the precipitate(s) formed, ~100 mg of Ag powder was added to the 1M HCl solution which was kept warm and stirred for ~3 min to remove Po. The sample was centrifuged and the supernate was transferred into an electroplating apparatus consisting of a 9 mm inner diameter glass chimney mounted on a plastic gasket above a Ni foil. The plating apparatus was warmed on a hot plate while the solution was mixed with a small Teflon coated magnetic stirring bar for ~5 min. Bismuth was removed from solution by self-deposition on the Ni foil. After removing the solution, the Ni foil was washed with 1M HCl. The foil was dried and mounted on an Al plate for counting. The chemical procedure took an average of 14 min and gave Bi yields of 60—80%.

C. Measurement of alpha-activity and data analysis

The radiochemically separated Bi samples were measured with an α-spectrometer system consisting of four independent Si(Au) surface barrier detectors allowing four samples to be counted simultaneously. Counting of a sample was typically started 20—30 min after the end of an irradiation and continued for a period of several hours. Data were stored in an event by event mode, each event being tagged by detector identification, event time, and energy.

The sample plates faced the detectors in a very close geometry, the solid angle subtended by the detector being about 5 sr. As a result, because of β-α summation, absorption in the source, and the dead layer of the detector, the overall α energy resolution was poor (FWHM ≃80

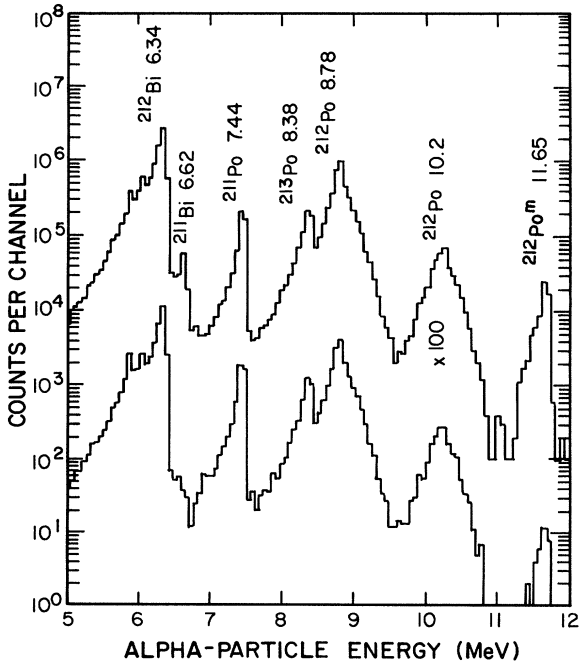

FIG. 1. Two consecutive 30-min α-particle spectra resulting from bombardment of a ^{208}Pb target with 152 MeV ^{18}O ions. The chemical procedure outlined in the text was used to separate Bi isotopes immediately following a 28 min irradiation. The counting of the sample was started 21 min after the end of the irradiation. Major α groups are labeled by the parent isotope and associated α-particle energy.

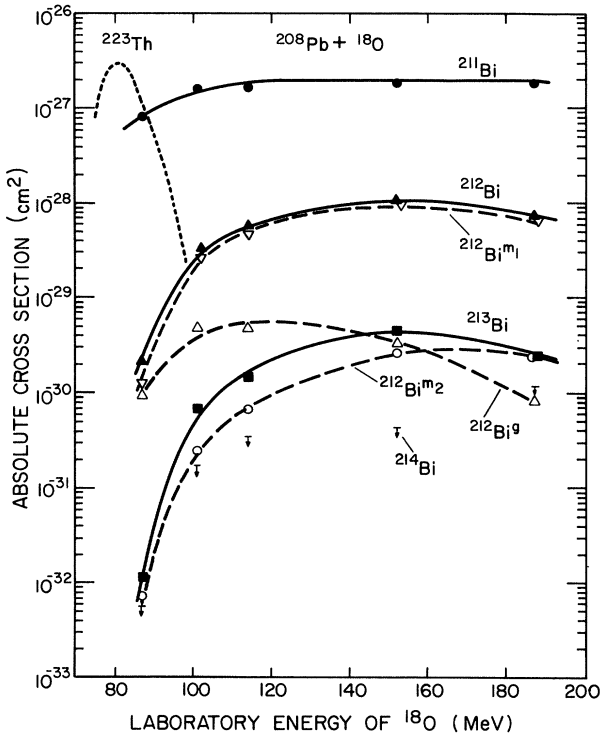

FIG. 2. Measured absolute cross sections for production of ^{211}Bi (●), ^{212}Bi (▲), and ^{213}Bi (■) in bombardment of ^{208}Pb by ^{18}O ions. The three dashed curves give the individual excitation curves for the ground state (△), the $J^\pi = 9^-$ isomer (▽), and the $J^\pi = 15^-$ isomer (○) of ^{212}Bi. The dotted curve shows the shape of the excitation function of the compound nuclear reaction ^{208}Pb(^{18}O,3n)^{223}Th for comparison (Ref. 16) (not in absolute scale). The arrows indicate observed upper limits for production of ^{214}Bi. Overall errors are estimated to be ≤50% for all points (see the text for additional discussion).

keV) and varied somewhat from sample to sample. A typical α-particle spectrum is presented in Fig. 1. The α-particle spectra were dominated by α activity from decay of Bi (Po) isotopes. However, in most of the samples, some contamination from the 7.2 h ^{211}At and its daughter nuclide ^{211}Po was present. The 7.44 MeV α group of ^{211}Po then reduced the sensitivity for detection of the 7.68 MeV α group of ^{214}Po, the β-decay daughter of 19.8 min ^{214}Bi. We found no conclusive evidence of the presence of ^{214}Bi in our samples.

The absolute cross sections were calculated by integrating the peak intensities in all counting intervals in which they were clearly observed. These data were then decay curve analyzed to obtain the half-lives and production yields. The integrated current was averaged over the period of the irradiation and transformed into a particle fluence by correcting for the charge state of the accelerated ion.

Because the 2.15 min half-life of ^{211}Bi was short relative to the time between the end of an irradiation and the beginning of the counting, ^{211}Bi was only seen in ^{208}Pb bombardments where it had a high abundance. In the estimation of upper limits of cross sections a limit of three times the standard deviation of the number of counts in the pertinent energy interval was used. Results of the cross section measurements are presented graphically in Figs. 2–4. The overall uncertainties in the measured cross sections are estimated to be less than 50% and are composed of the following incoherent factors: counting statistics $\lesssim$20%, target thickness and beam integration $\lesssim$20%, chemical yield $\lesssim$10%, alpha particle counting efficiency for the closely mounted diffuse samples $\lesssim$20%, beam intensity fluctuations and timing uncertainties (only applicable for the short lived ^{211}Bi) $\lesssim$20%. Error bars are not included in Figs. 2–4 to avoid unnecessary cluttering but the scatter of the experimental points are consistent with our overall error estimate. Conclusions drawn from the extracted cross section values are not affected by variation of measured values within estimated error limits. The laboratory energies of ^{18}O ions are average energies at the target corrected for energy losses in the Havar window, cooling gas, and in the target itself. The corrections ranged from 7 to 12 MeV.

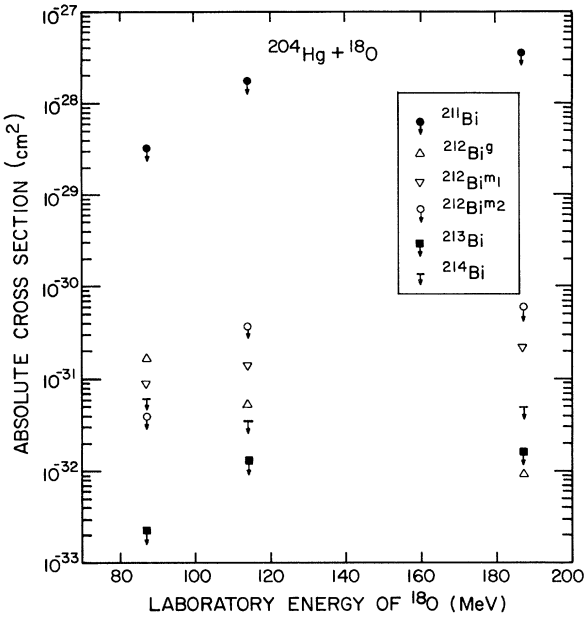

FIG. 4. Measured absolute cross sections or upper limits of cross sections for production of Bi isotopes (A =211 to 214) in bombardments of ^{204}Hg by ^{18}O ions. The symbols have the same meanings as in Figs. 2 and 3. Overall errors are estimated to be $\lesssim$50% for all points (see the text for additional discussion).

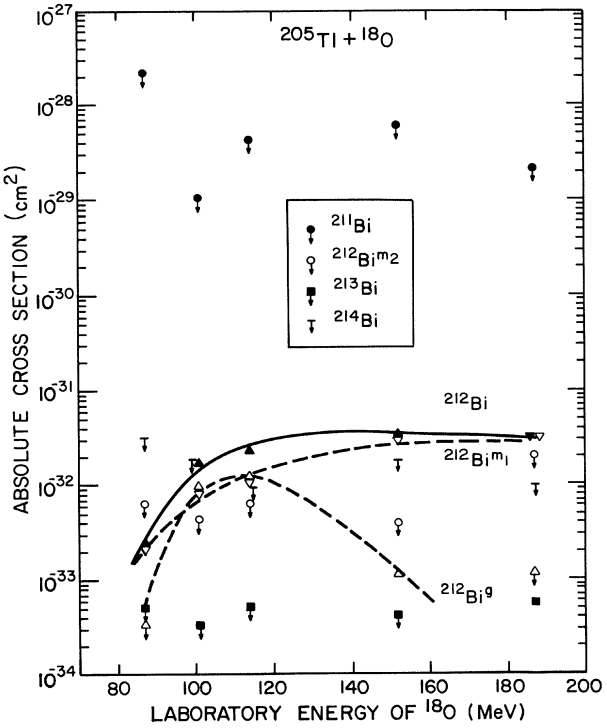

FIG. 3. Measured absolute cross sections or upper limits of cross sections for production of Bi isotopes (A =211 to 214) in bombardments of ^{205}Tl by ^{18}O ions. The symbols have the same meaning as in Fig. 2. The symbols with downward pointing arrows mark an upper limit based on counting statistics. Overall errors are estimated to be $\lesssim$50% for all points (see the text for additional discussion).

Our measured absolute cross sections for production of the ground state ($J^{\pi}=1^{-}$) and two isomeric states ($J^{\pi}=9^{-}$ and 15^{-}) of ^{212}Bi also provide isomer ratios σ_{m_1}/σ_g, σ_{m_2}/σ_g, and $\sigma_{m_2}/\sigma_{m_1}$ as a function of the bombardment energy. The isomer ratios resulting from bombardments of ^{208}Pb with ^{18}O are presented in Fig. 5. It is seen that both σ_{m_1}/σ_g and σ_{m_2}/σ_g increase rapidly and smoothly as a function of the projectile energy. As a result of the similar behavior of these two ratios, $\sigma_{m_2}/\sigma_{m_1}$ increases relatively slowly as a function of energy. It is to be noted that even at the highest bombarding energy the ratio $\sigma_{m_2}/\sigma_{m_1}$ is only about 0.04, implying a rather low angular momentum in ^{212}Bi. Because of the poorer counting statistics in Tl and Hg bombardments the isomer ratios of ^{212}Bi are presented only at a couple of bombarding energies and these values have large statistical errors.

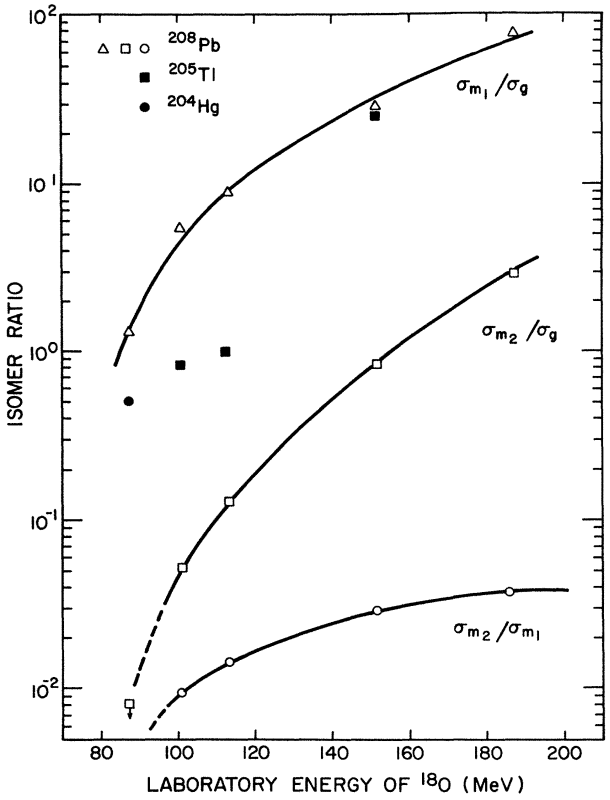

FIG. 5. The experimental isomer ratios for the $J^{\pi}=9^{-}$ (m_1) and $J^{\pi}=15^{-}$ (m_2) states of ^{212}Bi plotted as a function of the ^{18}O projectile energy. The points joined by eye-guiding lines are associated with bombardments of ^{208}Pb targets. The individual points relate to ^{205}Tl (■) and ^{204}Hg (●) targets, and measured values of the ratio σ_{m_1}/σ_g. Isomer ratio uncertainties are estimated to be $\leq 20\%$ for the ^{208}Pb bombardments and $\leq 50\%$ for the ^{205}Tl and ^{207}Hg targets.

III. RESULTS AND DISCUSSION

A. Decay of the 9^{-} isomer of ^{212}Bi

Baisden *et al.*[4] discovered the 25 min ($J^{\pi}=9^{-}$) and 9 min ($J^{\pi}=15^{-}$) isomers in ^{212}Bi. The decay properties of these isomeric states were only investigated by α-decay studies. Subsequently, Lemmertz *et al.*[5] performed a detailed study of the decay of the 9^{-} isomer to levels of ^{212}Po by means of α-γ spectroscopy. Relative decay branches for direct α-emission leading to levels of ^{208}Tl, for β-delayed α emission from excited states of ^{212}Po to ^{208}Pb, and for β-delayed γ emission to the ground state of ^{212}Po were not given in either of the previous studies of the decay of the $J^{\pi}=9^{-}$ ^{212}Bi. Because the knowledge of the branching ratios was necessary for the determination of both the production cross section of ^{212}Bi and of the isomeric ratios, an effort was made to extract the branching ratios from the measured data. Due to poor energy resolution in the measured α-particle spectra close lying α peaks could not be resolved.

An analysis of the multiple peak at 6.3 MeV and the structure below resulted in assignment of four α peaks with energies (and intensities) of 6.34 (35±1%), 6.30 (26±1%), 6.01 (5±1%), and 5.75 (0.5±0.2%) MeV to the decay of the $J^{\pi}=9^{-}$ state to levels of ^{208}Tl. The ratio of the intensity of the two stronger peaks was taken from the work of Baisden *et al.*[4] The intensity of the two weaker peaks are relative to the sum of the 6.34 and 6.30 MeV peak being 61%. These two less intense peaks represent hitherto unobserved fine structure in the α decay of the isomer. It appears that the 6.01 MeV peak is also clearly visible, although unassigned, in the α spectrum presented by Lemmertz *et al.*[5] Branchings of (67±1)%, (30±1)%, and (3.2±0.2)% were obtained for direct α decay to levels of ^{208}Tl, for β-delayed α emission to ^{208}Pb, and for β-delayed γ emission leading to the ground state of ^{212}Po. These values are based on the observed ratio of counts in the multiple α peak at 6.3 MeV, in the energy interval 9.6–10.9 MeV and in the 8.78 MeV peak. The contribution of the decay of the 60.6 min ^{212}Bi to the 8.78 MeV peak was eliminated by taking the difference of two consecutive 75 min spectra, the latter spectrum being multiplied by a factor of 2.36 to allow for the decay of the 60.6 min component. The half-lives of the $J^{\pi}=9^{-}$ and 15^{-} isomeric states were measured to be 25.0±0.2 min, and 7.0±0.3 min, respectively. A schematic decay scheme of ^{212}Bi including information pertinent to this study is presented in Fig. 6.

Low lying excited states of ^{212}Bi are most likely to be

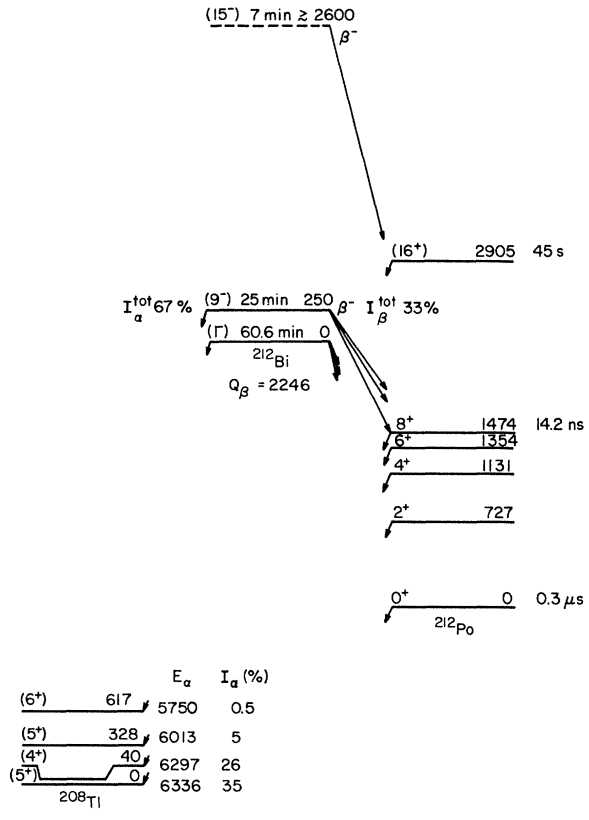

FIG. 6. Schematic decay scheme of ^{212}Bi. Only details pertinent to this study are presented. All energies are given in keV. The location of the shown levels of ^{208}Tl has been shifted upwards relative to those of ^{212}Bi and ^{212}Po for convenience.

dominated by the $(\pi 1h_{9/2})(\nu 2g_{9/2})$ configuration. This is known to be the case for ^{210}Bi, in which all the members of this n-p multiplet have been found to appear as dominant configurations in one of the nine lowest-lying levels.[6] Thus the $J^\pi=9^-$ isomeric state of ^{212}Bi is characterized by the $(\pi 1h_{9/2})(\nu 2g_{9/2})_{9^-}(\nu 2g_{9/2})^2_{0^+}$ configuration, as suggested by Baisden *et al.*[4] A conversion of this configuration by a $g_{9/2}$ neutron to $h_{9/2}$ proton transition would lead to the $(\pi 1h_{9/2})^2_{8^+}(\nu 2g_{9/2})^2_{0^+}$ configuration of ^{212}Po assuming a first-forbidden unhindered β transition. The logft value associated with this transition could be used as a measure of the purity of the suggested initial and final configurations. Unfortunately, because detailed information on the α- and γ-decay widths of the pertinent excited states of ^{212}Po is lacking, β-decay branchings to individual states cannot be deduced from the available data. However, on the basis of our measured value (33.2%) of the total β branching to levels of ^{212}Po from the 9^- isomer of ^{212}Bi, we can set a lower limit log$ft=5.9$ to a β transition leading to the $J^\pi=8^+$, 1474-keV level of ^{212}Po. A logft value of this magnitude is rather close to other similar transitions, e.g., the ground state β transitions of ^{209}Pb (log$ft=5.5$) and ^{211}Bi (log$ft=6.0$). If one assumes that the β transition from the $J^\pi=15^-$ isomer of ^{212}Bi to the $J^\pi=16^+$ isomer of ^{212}Po also has a logft of 6.0, the $J^\pi=15^-$ state should be at about 2.65 MeV above the ground state of ^{212}Bi. This could be taken as a lower limit on its excitation energy, unless the main decay channel of the isomer is other than the said β transition.

The β-delayed α emission from the excited states of ^{212}Po seems to be worthy of a more detailed study. It is unique because β decay from three long-lived states of ^{212}Bi with widely different spin values (1^-, 9^-, and 15^-) feed excited states of ^{212}Po. Detailed α-γ spectroscopic study should yield life times as well as α- and γ-decay widths of pertinent excited states. As a result one would have a set of excited states of widely different nature feeding a well defined final state, the ground state of ^{208}Pb. These data should be of great value in application of shell model calculations to α decay in the vicinity of the doubly closed shell.

B. Isomer ratios

The observed isomer ratios are directly related to the excitation energy (E) and angular momentum (J) distributions in the (E,J) space prior to γ-ray cascade leading to one of the three long-lived states in ^{212}Bi. Because we do not have an adequate understanding of the reaction mechanisms leading to production of ^{212}Bi in its different states, a detailed calculation of isomer ratios on the basis of (E,J) distributions at various stages of the process leading to the final states of ^{212}Bi is unwarranted. However, a useful framework for a qualitative discussion of the observed isomer ratios is provided by the "sum rule model" of Wilczyński *et al.*[7,8] The calculations based on this model were done using the program coded by Beene at Oak Ridge National Laboratory.[9,10]

The calculated angular momentum distributions and average angular momentum values for the incomplete fusion reactions ^{208}Pb(^{18}O,^{14}N)^{212}Bi and ^{208}Pb(^{18}O,^{13}N)^{213}Bi are presented in Fig. 7. It is seen that according to the model only a relatively narrow window of J values dominates at a given energy. This is because lower l values are almost fully exhausted by the complete fusion channel, while the critical angular momentum value l_{cr} for fusion of the target and the captured fragment sets an upper limit at high l values. Empirical evidence for localization of incomplete fusion reactions in l space has been deduced from γ-ray multiplicity measurements in coincidence with charged particles associated with a given reaction channel.[8,11]

Of all the states populated in ^{212}Bi only the ones that lie roughly between the yrast line $E_y(J)$ and the entry line defined by $E_e(J)=E_y(J)+B_n$ will eventually decay either to the ground state or the two isomeric states. The availability of many high spin proton and neutron orbitals close to the Fermi level gives rise to a large number of low-lying, high-spin states in ^{212}Bi. This can be concluded on the basis of the observed level structure in the neighboring odd-odd isobaric nuclide ^{212}At (Ref. 12) or by consideration of coupling an odd neutron in one of the orbitals $g_{9/2}$, $i_{11/2}$, or $j_{15/2}$ to states in ^{211}Bi.[13] The yrast line in ^{212}Bi may thus be expected to rise relatively slowly as a

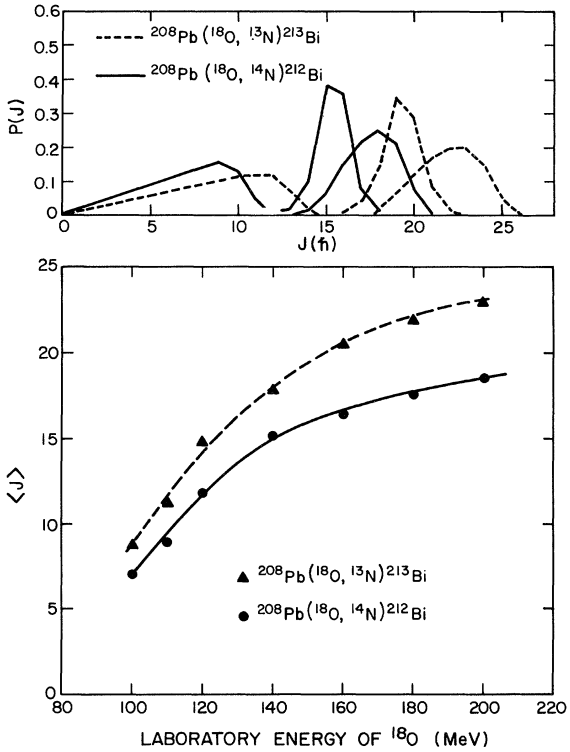

FIG. 7. In the upper part the calculated angular momentum distributions prior to particle emission for the binary reactions ^{208}Pb(^{18}O,^{14}N)^{212}Bi (solid curves) and ^{208}Pb(^{18}O,^{13}N)^{213}Bi (dashed curves) are plotted for projectile energies of 100, 140, and 180 MeV. In the lower part average angular momentum values $\langle J\rangle$ for the same reactions are plotted as a function of projectile energy. The following values were used for the empirical model parameters: $T=3.5$ MeV, $R_c/(A_1^{1/3}+A_2^{1/3})=1.5$ fm and $\Delta=2.0\hbar$ (Ref. 8).

function of J and states of $J=20\hbar$–$25\hbar$ should be available at about 3–4 MeV. The neutron binding energy of ^{212}Bi is 4.34 MeV. The population of the isomer depends on reaching a sufficient spin while still maintaining an excitation energy at that angular momentum so as to preclude neutron emission. Thus the region of population for the three long-lived states in ^{212}Bi is a relatively narrow zone in the E-J plane.

Let us assume that the J distributions depicted in Fig. 7 roughly represent the entry state angular momentum distributions. The statistical γ-ray cascade will broaden the spin distributions and shift the distribution in the direction of J values with the highest level density. The overall effect is for the sharply peaked J distributions to spread out slightly with an overall shift to lower J values. The rapid rise of the σ_{m_1}/σ_g and σ_{m_2}/σ_g as a function of the projectile energy is consistent with the fast increase in the average angular momentum brought into the system. However, on the basis of the calculated J distributions one would expect that at higher bombarding energies σ_{m_2} would exceed σ_{m_1} whereas the maximum observed ratio of $\sigma_{m_2}/\sigma_{m_1}$ value is only 0.04. The states corresponding to the higher upper tail of the J distribution are at, or close to, the yrast line and deexcite by a cascade of γ rays through yrast states. The actual population of the $J^\pi=15^-$ isomeric state depends on the relative number of the cascades reaching the yrast line with $J \gtrsim 15\hbar$. In addition, the relative population of this state may also critically depend on the availability and location of other discrete levels with $J=15$ or 15 ± 1 at about the same excitation.[14,15]

C. Reaction cross sections

A large number of both experimental and theoretical studies of cross sections for heavy ion induced multinucleon transfer reactions have been carried out during the last few years (see, e.g., recent review papers[17,18]). Much attention has been paid to binary processes, in which projectilelike and targetlike fragments are formed. These studies have focused on different aspects of incomplete fusion reactions, such as energy and angular distributions of the projectilelike particles,[19] excitation functions,[20,21] angular momentum transfer,[8,11] and associated light particle emission.[22] A number of models have been used to interpret the accumulated data. A commonly used model is the sum-rule model proposed by Wilczyński *et al.*[7] The model leads to definite predictions of absolute cross sections for all possible incomplete fusion channels and their localization in the l space as already discussed in Sec. III B.

Up to now most of the incomplete reaction studies have dealt with the major reaction channels and very little information is available about weak, highly asymmetric transfer channels of the type studied in this work. However, in a recent paper by Lee *et al.*,[21] excitation curves for production of heavy actinides from interactions of ^{18}O with ^{248}Cm and ^{249}Cf were measured. Although the observed peak cross sections for an effective transfer of the same number of protons and neutrons from the projectile to the target are rather comparable to our values there is a striking difference in the behavior of the excitation curves as a function of energy. In the actinide region the reaction cross sections reach their peak value typically some 20–30 MeV above the Coulomb barrier and then decrease steadily as the bombarding energy is increased. The rate of decrease seems to be roughly proportional to the number of transferred protons and the total number of transferred nucleons. In contrast, the cross section curves for production of Bi isotopes are relatively flat over the range studied. A possible cause for the seemingly different behavior of the cross sections at higher bombarding energies is the large difference in fission barrier heights. In the former, the barrier heights are typically 5–6 MeV (Ref. 23) and in the latter about 20 MeV,[24] with shell effects playing a dominant role in shaping the barriers in both cases. The critical question with regard to the heavy actinide region is what will happen to the fission barrier as a function of angular momentum. The underlying liquid drop will only decrease on the order of 0.5 MeV with spins even up to $20\hbar$ (Ref. 25) (greater than the spins implied for the isomer ratio analysis as discussed in Sec. II for the Bi isotopes). However, since the barrier is primarily shell stabilized, the more important question is how the shell effects vary with angular momentum. We do not have an explicit calculation of this quantity but believe it will vary among the heavy actinides and make precise predictions of the location of the production cross section maxima difficult.

The very different shape of the target nuclei in the Pb and Cf regions may also influence the reaction cross sections as suggested by recent experiments of Tricoire *et al.*[26] (see also Ref. 17) in which it was found that the localization of the entrance channel angular momentum window depends on the target deformation. An indication of such an effect may also be the large peak cross section, about 1.5 μb, for an effective transfer of ^{7}He to ^{249}Cf, while the peak cross section for the same transfer to ^{208}Pb is only about 0.04 μb.

The calculated sum rule cross sections[10] for the incomplete fusion reactions ^{208}Pb(^{18}O,$^{15-x}$N)$^{211+x}$Bi ($x=0$, 1, 2, and 3) are shown in Fig. 8. The predicted cross sections fall steeply when the calculated excitation energy of the residual nuclide exceeds the neutron binding energy. It is seen that the measured excitation functions (Fig. 2) do not behave as predicted, but stay relatively constant over the studied energy range. It is apparent that the sum rule model prediction cannot give a satisfactory explanation for the observed cross section data.

A comprehensive study of transfer reactions induced by heavy ions in ^{209}Bi has been carried out by Gardès *et al.*[20,27] They have measured excitation functions for the production of ^{210}Bi, ^{210}Po, ^{211}At, and ^{211}Rn corresponding to an effective transfer of 1n, 1p, 2p, and 3p-1n from the projectile to the target, respectively. All the excitation functions exhibit a sharp increase at low energy and a relatively constant value at high incident energy. The positions of the thresholds are strongly influenced by the reaction Q values. These experimental results are qualitatively similar to our results dealing with more complex reaction channels. The energetics can be character-

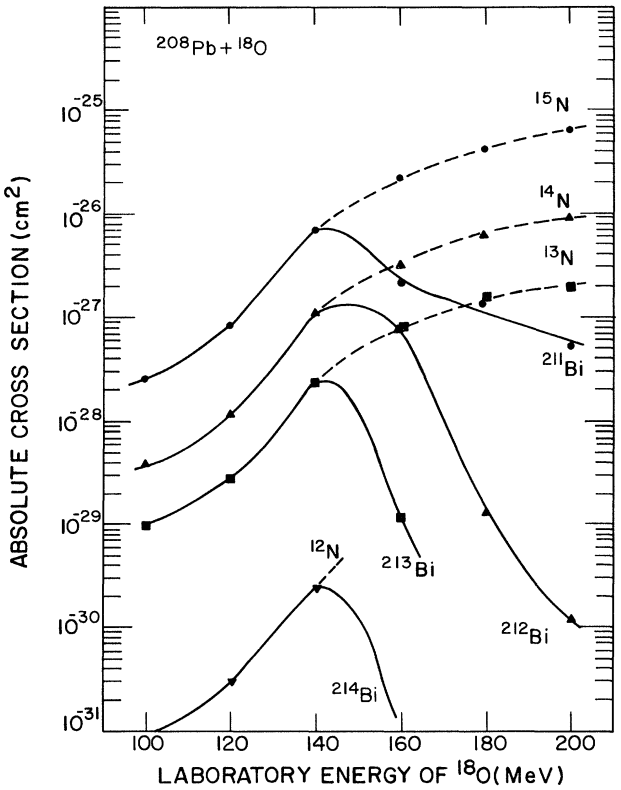

FIG. 8. The calculated "sum rule" cross sections for the ^{208}Pb(^{18}O,$^{15-x}$N)$^{211+x}$Bi ($x=0$, 1, 2, and 3) reaction (Ref. 10). The dashed curves indicate the calculated cross sections prior to particle evaporation from the excited targetlike fragment.

ized by the expression $Q_{gg}-\Delta B$, where Q_{gg} is the mass balance in the reaction and $\Delta B=V_f(R)-V_i(R)$ is the difference between the maxima of the interaction potentials in the exit and entrance channels. The values of $Q_{gg}-\Delta B$ are given in Table I for reaction channels leading to $^{211-214}$Bi nuclides from ^{204}Hg, ^{205}Tl, and ^{208}Pb targets. The interaction potentials $V(R)=V_C(R)+V_N(R)$, where $V_C(R)$ and $V_N(R)$ are the Coulomb and nuclear potentials ($r_0=1.0$ fm, $V_0=-30$ MeV),[28] were used to calculate the $Q_{gg}-\Delta B$ values. The effect of increasingly negative $Q_{gg}-\Delta B$ values for the ^{208}Pb(^{18}O,$^{15-x}$N)$^{211+x}$Bi reactions with $x=0$, 1, 2, and 3 causes a shift of reaction thresholds upwards in energy as seen from Fig. 2. The fact that only an upper limit was observed for production of ^{214}Bi is consistent with the highly negative $Q_{gg}-\Delta B$ value.

TABLE I. Values of the expression $Q_{gg}-\Delta B$, in MeV for the reaction channels leading to $^{211-214}$Bi.

Target \ Product	^{211}Bi	^{212}Bi	^{213}Bi	^{214}Bi
^{208}Pb	−2.1	−8.9	−14.7	−31.2
^{205}Tl	4.0	−10.8	−19.2	−36.7
^{204}Hg	3.5	−3.9	−7.6	−22.5

Gardès *et al.*[20] explain the constant cross sections observed for the high energy part of excitation functions by assuming that the optimum distance of approach,

$$R_{\text{opt}}=r_0(A_1^{1/3}+A_2^{1/3}),$$

is independent of energy for the higher bombarding energies. The range of R values, ΔR, for which the transfer probability is significant is also taken to be constant. In addition, the shape and amplitude of the transfer probability for a partial wave l are taken to be independent of incident energy. With these assumptions the cross section for a given transfer reaction can be written in the form

$$\sigma(\bar{E})=P(l)\pi\lambda^2\sum_{l_1}^{l_2}2(l+1),$$

where $\bar{E}$ is the c.m. incident energy and l_1 and l_2 are the l values corresponding to the edges of the R window, ΔR. The above discussed two concepts: the energy balance of the reaction at the distance of approach where the transfer occurs, and the optimum distance of approach for transfer, are quite successful in explaining the behavior of

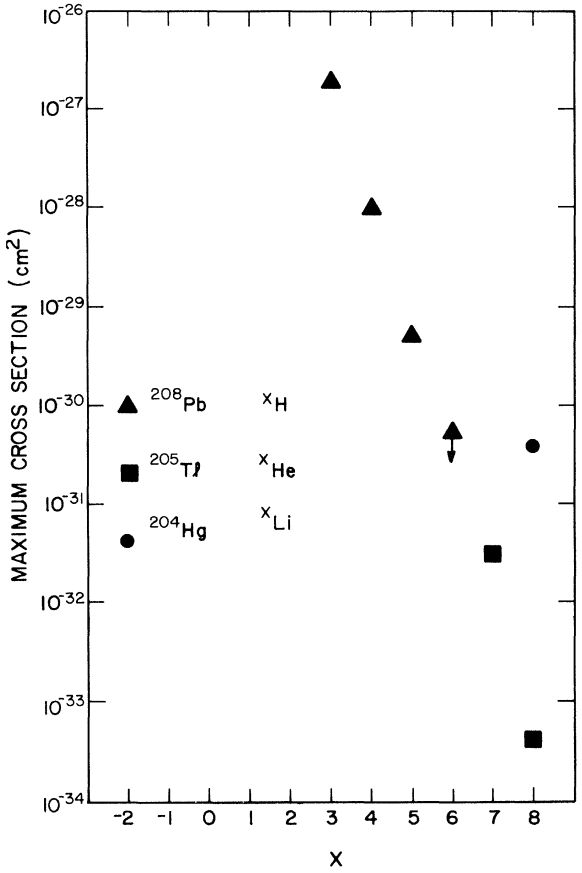

FIG. 9. The observed maximum cross sections for an effective transfer of X nucleons from the projectile to the target for ^{18}O induced transfer reactions on ^{208}Pb, ^{205}Tl, and ^{204}Hg targets. The arrows indicate measured upper limits. The symbols refer to various targets and effective particle transfers as indicated in the figure.

the observed cross sections at low incident energies and also the appearance of the "high energy plateau" for the reactions studied by Gardès *et al.*[20] The same qualitative features are apparent also in the case of the more complex transfer reactions studied in this work. However, a sliding l window that maintains the constant cross section may not be consistent with the low angular momentum transfer inferred from our observed isomer production ratios. The large variations of absolute cross sections for individual reactions could in the above model be associated with a dependence of the $P(l)$ factors on other parameters characterizing the transfer reactions, e.g., the effective number X of nucleons transferred from the projectile to the target nucleus. The dependence of the transfer reaction cross sections on X has been discussed by Karp *et al.*[19] and by Lee *et al.*[21,29] for reactions of the type under discussion. In Fig. 9, we present as a function of X the maximum cross sections for transfer reactions studied in our experiment. The dependence of the cross sections on X show, in general, a rapid decrease in yield with increasing mass transfer. However, other variables beside X can be important in determining the yield. We note the ^{8}Li transfer cross section is $\sim$500 times greater than the ^{8}He transfer. This increased yield could be due to the more favorable energetics, as presented in Table I, of the ^{8}Li ($Q_{gg}-\Delta B = -3.9$) vs that for ^{8}He ($Q_{gg}-\Delta B = -14.2$). The general rapid decrease is similar to what has been observed in the ^{18}O reaction with ^{248}Cm, ^{249}Cf, and ^{254}Es.[21,29] However, as pointed out previously, the cross section for (2p,5n) transfer and possibly also for other (2p,xn) transfers are much larger for a ^{249}Cf target than for a ^{205}Tl target. This puzzling feature is, of course, beneficial for production of neutron excess actinides.

IV. CONCLUSION

These experiments have demonstrated the viability of using the transfer mechanism to produce substantial quantities of neutron excess isotopes. The measured excitation functions are much flatter than predicted by, e.g., the sum rule model. Also the angular momentum transferred in these reactions as determined from isomer production ratios appears to be smaller than predicted by the model. The consequence of both the relatively high production yield and the low angular momentum are favorable for the production of neutron excess heavy actinides. Low residual excitation energy and angular momentum will help these systems survive fission decay competition.

ACKNOWLEDGMENTS

We wish to thank the operating staff of the 88-Inch Cyclotron at the Lawrence Berkeley Laboratory for their support during the irradiation phase of our experiments. We wish to acknowledge helpful discussions with J. R. Beene, H. C. Britt, D. C. Hoffman, and W. von Oertzen. K.E. and P.E. would like to thank The Finnish Cultural Foundation for travel grants. This work was funded by the U. S. Department of Energy.

---

*Permanent address: Department of Physics, University of Helsinki, Helsinki, Finland.

†Permanent address: Department of Theoretical Physics, University of Helsinki, Helsinki, Finland.

‡Permanent address: The Squibb Institute for Medical Research, P.O. Box 191, New Brunswick, NJ 08903.

[1]D. C. Hoffman, J. B. Wilhelmy, J. Weber, W. R. Daniels, E. K. Hulet, R. W. Lougheed, J. H. Landrum, J. F. Wild, and R. J. Dupzyk, Phys. Rev. C 21, 972 (1980).

[2]E. K. Hulet, R. W. Lougheed, J. H. Landrum, J. F. Wild, D. C. Hoffman, J. Weber, and J. B. Wilhelmy, Phys. Rev. C 21, 966 (1980).

[3]J. F. Wild, E. K. Hulet, R. W. Lougheed, P. A. Baisden, J. H. Landrum, R. J. Dougan, and M. G. Mustafa, Phys. Rev. C 26, 1531 (1982).

[4]P. A. Baisden, R. E. Leber, M. Nurmia, J. M. Nitschke, M. Michel, and A. Ghiorso, Phys. Rev. Lett. 41, 738 (1978).

[5]P. Lemmertz, L. J. Alquist, R. Fass, H. Wollnik, D. Hirdes, H. Jungclas, R. Brandt, D. Schardt, and J. Zylicz, Z. Phys. A 298, 311 (1980).

[6]W. W. Daehnick, M. J. Spisak, and J. R. Comfort, Phys. Rev. C 23, 1906 (1980).

[7]J. Wilczyński, K. Siwek-Wilczyńska, J. van Driel, S. Gonggrijp, D. C. J. M. Hageman, R. V. F. Janssens, J. Lukasiak, and R. H. Siemssen, Phys. Rev. Lett. 45, 606 (1980).

[8]J. Wilczyński, K. Siwek-Wilczyńska, J. van Driel, S. Gonggripj, D. C. J. M. Hageman, R. V. F. Janssens, J. Lukasiak, R. H. Siemssen, and S. Y. van der Werf, Nucl. Phys. A373, 109 (1982).

[9]J. R. Beene, M. L. Halbert, D. C. Hensley, R. A. Dayras, K. Geoffrey Young, D. G. Sarantites, and J. H. Barker, Phys. Rev. C 23, 2463 (1981).

[10]J. R. Beene (private communication).

[11]K. A. Geoffroy, D. G. Sarantites, M. L. Halbert, D. C. Hensley, R. A. Dayras, and J. H. Barker, Phys. Rev. Lett. 43, 1303 (1979).

[12]T. Lönnroth, V. Rahkonen, and B. Fant, Nucl. Phys. A376, 29 (1982).

[13]B. Silvestre-Brac and J. P. Boisson, Phys. Rev. C 24, 717 (1981).

[14]G. Liggett and D. Sperber, Phys. Rev. C 3, 447 (1971).

[15]H. Groening, K. Aleklett, K. J. Moody, P. L. McGàughey, W. Loveland, and G. T. Seaborg, Nucl. Phys. A389, 80 (1982).

[16]K. Eskola, Phys. Rev. C 5, 942 (1972).

[17]C. Gerschel, Nucl. Phys. A387, 297c (1982).

[18]R. H. Siemssen, Nucl. Phys. A400, 245c (1983).

[19]J. S. Karp, S. G. Steadman, S. B. Gàzes, R. Ledoux, and F. Videbaek, Phys. Rev. C 25, 1838 (1982).

[20]D. Gardès, R. Bimbot, J. Maison, L. de Reilhac, M. F. Rivet, A. Fleury, F. Hubert, and Y. Llabador, Phys. Rev. C 18, 1298 (1978).

[21]D. Lee, K. J. Moody, M. J. Nurmia, G. T. Seaborg, H. R. von Gunten, and D. C. Hoffman, Phys. Rev. C 27, 2656 (1983).

[22]R. K. Bhowmik, J. van Driel, R. H. Siemssen, G. J. Balster, P. B. Gold, S. Gonggrijp, Y. Iwasaki, R. V. F. Janssens, H. Sakai, K. Siwek-Wilczyńska, W. A. Sterrenburg, and J. Wilczyńska, Nucl. Phys. A390, 117 (1982).

[23]H. C. Britt, E. Cheifetz, D. C. Hoffman, and J. B. Wilhelmy,

Phys. Rev. C 21, 761 (1980).
[24]L. G. Moretto, S. G. Thompson, J. Routti, and R. C. Gàtti, Phys. Lett. 38B, 471 (1972).
[25]S. Cohen, F. Plasil, and W. J. Swaitecki, Ann. Phys. (N.Y.) 82, 557 (1974).
[26]H. Tricoire, C. Gerschel, N. Perrin, H. Sergolle, L. Valentin, D. Bachelier, H. Doubre, and J. Gizon, Z. Phys. A 306, 127 (1982).
[27]D. Gardès, R. Bimbot, J. Maison, M. F. Rivet, A. Fleury, F. Hubert, and Y. Llabador, Phys. Rev. C 21, 2447 (1980).
[28]C. Ngo, B. Tamain, M. Beiner, R. J. Lombard, D. Mas, and H. H. Deubler, Nucl. Phys. A252, 237 (1975).
[29]D. Lee, H. von Gunten, B. Jacak, M. Nurmia, Y.-F. Liu, C. Luo, G. T. Seaborg, and D. C. Hoffman, Phys. Rev. C 25, 286 (1982).